REVISION 1

A critical comment on Ertl et al. (2012): *"Limitations of Fe^{2+} and Mn^{2+} site occupancy in tourmaline: Evidence from Fe^{2+}- and Mn^{2+}-rich tourmaline"*

FERDINANDO BOSI AND GIOVANNI B. ANDREOZZI

[1]Dipartimento di Scienze della Terra, Sapienza Università di Roma, Piazzale Aldo Moro, 5, I-00185 Rome, Italy

We dedicate this paper to the memory of Prof. Sergio Lucchesi who spent his life working to promote the diffusion of correct scientific information

ABSTRACT

In this paper we have presented a detailed response to Ertl et al. (2012a) who, in a recent paper in this journal, claim evidence for limitations of Fe^{2+} and Mn^{2+} occupancy at the Z site of the tourmaline structure. They also propose a model by which the <Z-O> distance of tourmaline varies as a function of its <Y-O> and <T-O> bond lengths. We have examined their conclusions and find that a different distribution of cations over the Y and Z sites gives better agreement with the extensive experimental information available. In fact, on the basis of crystal-structure refinements, Mössbauer spectroscopy, optical absorption spectroscopy, bond-valence theory, ionic radius concept and literature, the occurrence of Fe^{2+} at the Z site of tourmaline is well supported. Conversely, existing experimental data does not provide indisputable evidence for the occurrence of Mn^{2+} at the Z site. In spite of this, there is no evidences for inductive effects of $^{Y}Mn^{2+}$ on <Z-O>, and the proposed effects must be regarded as speculative. Statistical analysis shows that the $<^{Z}$Al-O> average value is 1.906(2) Å, which is consistent with the observed values of $<^{Z}$Al-O> at the 99% confidence limit (within 3σ) in tourmalines with the Z site fully occupied by Al. Consequently, the proposed inductive effect of <Y-O> and <T-O> on <Z-O> can be ruled out.

INTRODUCTION

In a recent publication in the American Mineralogist, Ertl et al. (2012a) reported experimental results which they interpret as definitive evidence that Fe^{2+} occurs only at the Y site in the tourmaline structure. Our analysis of the extensive available experimental information suggests that significant amounts of Fe^{2+} can be found at the Z site (see below). In addition, we will show that the apparent correlation between the average <Z-O> and <Y-O> (or <T-O>) bond distances which Ertl et al. (2012a) ascribe to an inductive effect is an artefact of the way they selected their statistical sample.

The tourmaline supergroup minerals are widespread borosilicates, occurring in sedimentary, igneous and metamorphic rocks. In accordance with Henry et al. (2011), the general formula of tourmaline may be written as: $XY_3Z_6T_6O_{18}(BO_3)_3V_3W$, where $X = Na^+$, K^+, Ca^{2+}, □ (=vacancy); $Y = Al^{3+}$, Fe^{3+}, Cr^{3+}, V^{3+}, Mg^{2+}, Fe^{2+}, Mn^{2+}, Li^+; $Z = Al^{3+}$, Fe^{3+}, Cr^{3+}, V^{3+}, Mg^{2+}, Fe^{2+}; $T = Si^{4+}$, Al^{3+}, B^{3+}; $B = B^{3+}$; V (≡O3) = OH^{1-}, O^{2-}; W (≡O1) = OH^{1-}, F^{1-}, O^{2-}.

A BRIEF HISTORY ON Fe^{2+} AT THE Z SITE IN TOURMALINE

To our knowledge, the first experimental information on Fe^{2+} occupancy at Z originates from Mössbauer studies by Burns (1972) and Hermon et al. (1973). Later, Korovushkin et al. (1979), Kraczka et al. (1986), Ferrow et al. (1988, 1993), Ferrow (1994), Foit et al. (1989), Fuchs et al. (1995, 1998), Baksheev et al. (2010), and Gadas et al. (2012) interpreted their Mössbauer spectra of various tourmalines in terms of Fe^{2+} disordering over the Y and Z sites. Additional information on the occurrence of Fe^{2+} at Z comes from the structural studies of Fortier and Donnay (1975), Razmanova et al. (1983), Grice and Robinson (1989), Francis et al. (1999) and Ertl and Hughes (2002), which quantified such an occurrence up to 7% atoms/site (Table 1). Supplementary pieces of information on Fe^{2+} at Z come from the optical absorption studies of Smith (1978), Mattson and Rossman (1987), de Camargo and Isotani (1988) and Taran et al. (1993).

An explanation supporting Fe^{2+} at Z was suggested by Donnay and Barton (1972) on the idea of the mutual size adjustment required of the edge-sharing coordination polyhedra about Y and Z cations. Using short-range bond-valence constraints, Hawthorne (1996) predicted that in addition to (Mg,Al) disordering "*similar arguments apply to their (Fe^{2+},Fe^{3+}) analogues*". Such a prediction was recently confirmed by Bosi (2011). Again, in a general review on boron-bearing minerals, dealing with the tourmaline crystal-chemistry, Henry and Dutrow (1996)

stated that the Z site "*can contain significant amounts of the divalent cation Mg^{2+} and Fe^{2+}*". The end-member oxy-schorl $Na^{Y}(Al_2Fe^{2+})^{Z}(Al_5Fe^{2+})Si_6O_{18}(BO_3)_3(OH)_3O$ was defined by Hawthorne and Henry (1999) and successively modified by Henry et al. (2011) as $Na^{Y}(Al_3)^{Z}(Al_4Fe^{2+}_2)Si_6O_{18}(BO_3)_3(OH)_3O$. In this regard, however, it should be noted that an end member is an algebraic entity, not a mineral. Consequently, the occurrence of such an end-member does not ensure that it can occur as a mineral. On experimental basis, Bosi and Lucchesi (2004), Bosi et al. (2005a), Bosi (2008) Andreozzi et al. (2008) proposed a model in which Fe^{2+} may occur at Y and Z, and Filip et al. (2012) reported a thermally-driven study in which Fe^{2+} is disordered over the Y and Z sites.

Ertl et al. (2012a) focus their attention only on published studies lacking evidence for significant amounts of Fe^{2+} at the Z site (Dyar et al. 1998; Bloodaxe et al. 1999; Pieczka and Kraczka 2001, 2004; Kraczka and Pieczka 2000), and stated that these studies are in contrast to the studies of Bosi, Andreozzi and co-workers, but disregard much of the literature mentioned above.

INCONSISTENCIES IN THE TOURMALINE LITERATURE ON FE

Dealing with Fe^{2+} site assignment, Ertl et al. (2012a) stated that (p. 1410) "*assignment of the Fe^{2+} doublets to Y sites in the Dyar et al. (1998) paper was mainly based on the compelling theoretical models of Pieczka (1997), Pieczka and Kraczka (1997), and Pieczka et al. (1998), who used structural analyses and chemical composition as the basis for their models. They concluded that Fe^{2+} occupies only the Y site in the structure, and argued that previous assignment of Fe^{2+} to the Z site simply does not make crystallochemical sense*". The models of Pieczka (1997) and Pieczka and Kraczka (1997) are based on literature data, and their conclusions need to be analyzed carefully. First, some of the data used in the development of the model are questionable. For example, the cation distributions of Grice and Ercit (1993) samples are affected by large errors (see the comment below); the olenite of Gorskaya et al. (1982) displays erroneous Z-O bond distance (see Bosi and Lucchesi 2007); the chromdravite of Nuber and Schmetzer (1979) has significant compositional uncertainties (see Foit 1989). In detail, the amounts of $^{Z}Fe^{3+}$ reported by Grice and Ercit (1993) for samples 43167, 43293, Cross, 32008, and 43873 actually correspond indeed to $^{Z}Fe^{2+}$, as already pointed out by Bosi (2008). This can be easily verified by comparing total Fe^{2+} and Fe^{3+} atoms per formula unit (apfu) from the chemical analysis shown in their Table 2 with the cation distributions shown in their Table 5: e.g., for sample 43167, Fe^{2+}_{tot} = 0.70 apfu and Fe^{3+}_{tot} = 0.98 apfu; but $^{Y}Fe^{2+}$ =

0.21 and $^{Z}Fe^{2+}$ = 0.00 (total = 0.21 apfu), and $^{Y}Fe^{3+}$ = 0.97 and $^{Z}Fe^{3+}$ = 0.49 (total = 1.46 apfu). Moreover, the models of Pieczka (1997) and Pieczka and Kraczka (1997) optimize bond distances using <Y-O> and <Z-O> rather than ionic radii. This is not the optimal approach, because it is well known that the cation-to-anion distance is also a function of constituent anion radius, which can offset in mean bond distance by up to 0.012 Å (see Hawthorne et al. 1993). Finally, the Pieczka model was obtained by constraining the Z site to be fully occupied by Al, although the <Z-O> distance varies from 1.90 to 1.94 Å in the samples used. Such a variation may also reflect Al replacement by larger cations such as Mg without showing any sign in the refined effective scattering at the Z site. On these grounds, the Pieczka model reveals a large degree of uncertainty.

Another controversial point concerns Fe^{3+}/Fe_{tot} ratios of the crystals analyzed by synchrotron micro-X-ray absorption near-edge spectroscopy (SmX) by Bloodaxe et al. (1999). The same samples had been previously studied by Mössbauer Spectroscopy (MS) in Dyar et al. (1998), and showed significant variations: e.g., for sample Ru-T17-92, $\%Fe^{3+}_{MS}$ = 0 and $\%Fe^{3+}_{SmX}$ = 35; for sample HP 2-1, $\%Fe^{3+}_{MS}$ = 8 and $\%Fe^{3+}_{SmX}$ = 27. In spite of this inconsistency, Ertl et al. (2012a) invoked the support of both the studies of Dyar at al. (1998) and Bloodaxe et al. (1999) to corroborate the model of Pieczka, i.e., Fe^{2+} solely at Y.

EVIDENT CONTRADICTIONS IN THE PAPER OF ERTL ET AL. (2012A)

Ertl et al. (2012a) state that (p. 1411) "*a simple calculation of theoretical <Z–O> bond lengths shows that such occupancies with only $^{Z}Fe^{2+}$ in sample GRAS1, as modeled by Bosi (2008), seems unrealistic. For GRAS1, in which <Z-O> is determined to be 1.921 Å (Ertl et al. 2006b), an extrapolative calculation of the theoretical <Z-O> bond length […] and a (slightly simplified) refined occupancy of $^{Z}(Al_{5.6}Fe_{0.4})$, gives a theoretical value of <Z-O> = 1.916 Å for a completely Fe^{2+}-free Z site [i.e., $^{Z}(Al_{5.6}Fe^{3+}_{0.4})$], but 1.924 Å for a Fe^{3+}-free Z site [i.e., $^{Z}(Al_{5.6}Fe^{2+}_{0.4})$]*". It is obvious from a simple arithmetical consideration that the value of 1.921 Å measured for sample GRAS1 is closer to the ideal value of 1.924 Å, calculated for $^{Z}(Al_{5.6}Fe^{2+}_{0.4})$, than to the value of 1.916 Å, calculated for $^{Z}(Al_{5.6}Fe^{3+}_{0.4})$. In addition, it should be noted that using the ionic radii of Bosi and Lucchesi (2007), the ideal value of <Z-O> obtained for $^{Z}(Al_{5.6}Fe^{2+}_{0.4})$ is 1.922 Å, in excellent agreement with the measured one.

Ertl et al. (2012a) criticize the refined octahedral ionic radii for Fe^{3+} obtained by Bosi and Lucchesi (2007) and consequently their optimization model, stating that (p. 1411) "*Bosi et al. (2005b) and Bosi and Lucchesi (2007) gave values [$r_{Fe3+(Y)}$ = 0.697 Å, $r_{Fe3+(Z)}$ = in the*

range 0.705 to 0.698 Å], which are, however, considerably larger than the Shannon (1976) value of $r_{Fe3+(HS)}$ *= 0.645 Å [...] Interestingly, the optimized radius values for* Fe^{2+}, $r_{Fe2+(Y)}$ *= 0.778 Å and* $r_{Fe2+(Z)}$ *= 0.774 Å (Bosi and Lucchesi 2007), are in good agreement with the Shannon (1976) value of* $r_{Fe2+(HS)}$ *= 0.78 Å. These obvious contradictions are not addressed by either Bosi (2008) or Bosi and Lucchesi (2007)*". Actually, Bosi and Lucchesi (2007) dedicated a whole section of their paper ("*The ionic radii of Al and* Fe^{3+}") to the reasons why the ionic radius of Fe^{3+} can vary from 0.705 to the Shannon value of 0.645 Å. In addition, the robustness of both the ionic radii of Bosi and Lucchesi (2007) and their approach to the optimization of cation distributions is confirmed by another optimization procedure (i.e., that of Wright et al. 2000), which results in comparable cation distributions. Compare, for example, Table 3 of Bosi and Lucchesi (2007) with appendix A.4.3 of Lussier (2011); see Table 6 of Bosi et al. (2012a, 2013a); see also Table 2 of this paper.

Ertl et al. (2012a) state that the structural refinements of Bosi et al. (2005b) are affected by large errors. However, the same authors use the bond distances of Bosi et al. (2005b) to obtain their findings and extrapolate their models (see below, section on "Mn^{2+}-rich tourmalines").

Ertl et al. (2012a) state that the smallest acceptable peak width for a single line in a quadrupole doublet in ^{57}Fe Mössbauer spectroscopy cannot be less than 0.24-0.25 mm/s. However, the same authors fit their Mössbauer spectra using a quadrupole distribution with Lorentzian peak widths of 0.20 mm/s (see their Table 5).

Ertl et al. (2012a) state that the optical absorption spectra of samples drv18 and GRAS1 show a pair of bands corresponding to Fe^{2+} at about 770 nm in the **E****c** spectrum. However, such samples show no significant bands at 770 nm in **E****c** (Figs. 5 and 6 in Ertl et al. 2012a).

Ertl et al. (2012a) refined a significant negative value of the Flack *x* parameter (absolute-structure determination of the noncentrosymmetric tourmaline structure) for samples MNELB3 and MNELB3H: –0.10(2) and –0.12(2), respectively. However, according to Flack and Bernardinelli (2000), the *x* parameter has a physically meaningful range only for $-3u \le x \le (1 + 3u)$, where *u* is the standard uncertainty of *x*. Values of $x(u)$ lying outside this statistical range, as is the case for MNELB3 ($-0.10 < -3u = -0.06$) and MNELB3H ($-0.12 < -3u = -0.06$), indicate that there is some systematic error in the model or in the data (H.D. Flack, personal communication). Thus, there is significant systematic error in the data for both MNELB3 and MNELB3H. Ertl et al. (2012a) did not give any explanation for the negative Flack parameter

values they obtained. Furthermore, Ertl et al. (2012b) did not give any explanation for the negative Flack parameters [–0.33(6) and –0.38(6)] refined for two Fe-rich tourmalines.

INCONSISTENCIES IN THE STRUCTURAL FORMULA OF SAMPLE BLS1

To evaluate the quality of a structural formula, we may refer to the recommendations by Hawthorne (1996) "*In combination, SREF and chemical analysis can, in many cases, indicate which scattering species occupy which sites, provided the number of scattering species at each site does not exceed two and provided that the species have significantly different scattering powers. Again, use of these methods alone can lead to erroneous assignment of cations to specific sites (e.g., see discussion by Hawthorne et al. 1993). It is necessary to combine crystal-chemistry analysis with SREF and chemical analysis (and possibly spectroscopic methods) to arrive at a correct structure and formula. Mean bond-length versus ionic radius relations and bond-valence theory Brown (1981) are of particular importance in this regard. It is necessary to stress these points, as several conclusions and proposals of previous work can be shown to be untenable when all aspects (crystal structure, crystal chemistry and chemical composition) of the problem are considered*".

For sample BLS1, the following structural formula was reported by Ertl et al. (2012a): $^{X}(Na_{0.88}Ca_{0.07}K_{0.02}\square_{0.03})^{Y}(Fe^{2+}_{2.02}Al_{0.41}Mn^{2+}_{0.32}Fe^{3+}_{0.23}Zn_{0.02})^{Z}(Al_{4.82}Fe^{3+}_{0.78}Fe^{2+}_{0.23}Ti^{4+}_{0.14}Mg_{0.03})^{T}(Si_{5.92}Al_{0.08})O_{18}(BO_3)_3{}^{V}(OH)_3{}^{W}[O_{0.49}F_{0.28}(OH)_{0.23}]$. Such a formula, however, is inconsistent from both ionic-radius and bond-valence perspectives. This is clearly shown in Table 2, where the cation distribution at the Y and Z sites in sample BLS1 are analyzed in detail. In this table, bond valences are calculated using bond-valence parameters from Brown and Altermatt (1985), and significant mismatch (Δ) is encountered between observed and calculated mean atomic number ($\Delta_{Y\text{-man}} = -0.37$ and $\Delta_{Z\text{-man}} = 0.25$), as well as between observed and calculated mean bond distances ($\Delta_{<Y\text{-}O>} = -0.041$ Å and $\Delta_{<Z\text{-}O>} = 0.011$ Å). In addition, there is a clear violation of the valence-sum rule, i.e., the mismatch between the bond-valence sum and the respective mean formal valence ($\Delta_Y = 0.23$ v.u. and $\Delta_Z = -0.06$ v.u.). Moreover, the above structural formula is in contrast to the short-range bond-valence constrains around the O1(≡W) site of the tourmaline structure. Thus, Henry et al. (2011) suggest stable local arrangements for Li-free tourmaline as follows: $^{Y}(3R^{2+})$ or $^{Y}(R^{3+} + 2R^{2+})$ around $^{W}(OH+F)^{1-}$ and $^{Y}(3R^{3+})$ or $^{Y}(2R^{3+} + R^{2+})$ around $^{W}O^{2-}$ (Hawthorne 1996, 2002; Bosi 2010, 2011). This assignment means that the occurrence of 0.5 apfu of $^{W}O^{2-}$ has to be associated with the occurrence of 1.0-1.5 apfu of $^{Y}R^{3+}$. In spite of this, the structural formula of Ertl et al. (2012a) for sample BLS1 has only

196 0.64 apfu of R^{3+}-cations at the Y site. On these grounds, such a structural formula seems
197 incorrect. Furthermore, considerations about Ti^{4+} site allocation are reported in Appendix 1.
198 An alternative cation distribution for sample BLS1 may be obtained by using the
199 methods of Bosi and Lucchesi (2004; 2007) and Wright et al. (2000). The results of these two
200 independent approaches converge to very similar cation distributions (see Table 2), which
201 show larger amounts of both Fe^{2+} at Z and Fe^{3+} at Y than those presented by Ertl et al. (2012a).
202 The new structural formulae show excellent agreement between calculated and observed data
203 (e.g., $\Delta_{Y\text{-man}} = 0.04$ and $\Delta_{Z\text{-man}} = 0.04$; $\Delta_{<Y\text{-}O>} = -0.002$ Å, $\Delta_{<Z\text{-}O>} = 0.001$ Å) and satisfy the
204 valence-sum rule ($\Delta_Y = 0.01$ v.u. and $\Delta_Z = 0.05$ v.u.). Moreover, they are fully consistent with
205 the short-range bond-valence constraints around the O1 site: about 1.3 apfu of $^{Y}R^{3+}$-cations
206 may now be associated with 0.5 apfu of $^{W}O^{2-}$.
207 As a conclusion, the cation distribution given by Ertl et al. (2012a) is not supported by
208 the crystal-chemical evidence or the chemical and crystallographic data that they presented.
209
210 **OPTICAL ABSORPTION SPECTROSCOPY**
211 Ertl et al. (2012a) presented optical absorption spectra of three Fe-bearing tourmalines
212 (samples BSL1, drv18 and GRAS1), and concluded that the recorded absorption bands near
213 720 and 1120 nm (BLS1) and 770 and 1160 nm (drv18 and GRAS1) in the **E**//**c** polarization
214 display no evidence of doubling, which would indicate Fe^{2+} occupancy at the Y and Z sites.
215 However, Ertl et al. (2012a) did not refer to published spectra and spectral interpretations that
216 indicate otherwise in other samples of tourmalines. For example, the studies of Smith (1978),
217 Mattson and Rossman (1987), de Camargo and Isotani (1988), and Taran et al. (1993)
218 converge to the conclusion that the bands at ~670 and ~1180 nm observed in the optical spectra
219 of some Fe-bearing tourmalines, are caused by Fe^{2+} at the Y and Z sites of the structure. In
220 detail, Ertl et al. (2012a) stated that the optical spectrum of sample BSL1 is comparable to that
221 of Mattson and Rossman (1987). However, Mattson and Rossman (1987) interpreted their
222 optical spectra in the **E**⊥**c** polarization by assigning the 670 nm band to Fe^{2+} at the Z site, and
223 the 765 nm band to Fe^{2+} at the Y site, with both sites absorbing at 1100 nm. We note that the
224 value of 720 nm recorded by Ertl et al. (2012a) for sample BLS1 is exactly intermediate
225 between those of $^{Z}Fe^{2+}$ and $^{Y}Fe^{2+}$, but they offer no comment to this.
226 Moreover, in support to their interpretation, Ertl et al. (2012a) presented an optical
227 spectrum of sample drv18. However, this spectrum shows a clearly asymmetric band close to
228 700 nm in the **E**⊥**c** polarization (Fig. 5 in Ertl et al. 2012a). This asymmetry strongly suggests

that at least two separate absorption bands contribute to this absorption feature, reflecting a "band doubling" most likely ascribable to Fe^{2+} at Y and Z. This band asymmetry is even more pronounced in the optical spectrum of sample GRAS1 (Fig. 6 in Ertl et al. 2012a). Such a **E**⊥**c** spectrum is extremely similar to that reported in Figure 11 by Mattson and Rossman (1987), who stated that the spectra "*exhibit an asymmetric 720 nm band which indicates two components*" (i.e., Fe^{2+} at Y and Z). As a conclusion, no evidence for the complete ordering of Fe^{2+} at the Y site in samples BSL1, drv18 and GRAS1 is provided.

MÖSSBAUER SPECTROSCOPY

Ertl et al. (2012a) considered the Mössbauer spectrum interpretation of Bosi (2008) to be uncertain because the peak width (Γ) for the doublet assigned to $^{Z}Fe^{2+}$ assignment is 0.53 mm/s. They stated that this is *"anomalously large"* and "*much greater than widths of other peaks that are closer to typical Γ values for silicates of ~0.26-0.30 mm/s*". Although this is correct in principle, inspection of real Mössbauer spectra reported in the literature (even restricting the analysis to tourmaline) offers several examples of peak widths up to 0.53 mm/s or even larger (see, for example, Mattson and Rossman 1984; Dyar et al. 1998; Pieczka and Kraczka 2004; Ertl et al. 2010a).

In the Appendix of Ertl et al. (2012a) a criticism of Mössbauer spectra interpretations offered by Andreozzi et al. (2008) is presented. The main concern is about the Fe^{2+} doublet with a quadrupole splitting (QS) of 1.38 mm/s, which was assigned by Andreozzi et al. (2008) to Fe^{2+} at the octahedrally-coordinated Z site on the basis of an integrated spectroscopic and structural approach. Ertl et al. (2012a) list a number of "*imprecisions*" which are hereafter examined according to their order of appearance.

1) As previously mentioned, Ertl et al. (2012a) stated that the smallest acceptable peak width in the Mössbauer spectroscopy for a single line in a quadrupole doublet cannot be below 0.24-0.25 mm/s. These values are, actually, the typically assumed lowest values for full-width at half-maximum of Lorentzian lineshapes in a Mössbauer spectrum. However, values somewhat lower may be observed in the literature, and this was not considered a problem (e.g., Dyar et al. 1998). In fact, the above mentioned values of 0.24-0.25 mm/s do not correspond to a physical limit, because it is well known that the natural line width of ^{57}Fe is about $5 \cdot 10^{-9}$ eV, corresponding to a minimum line width 0.194 mm/s for a Lorentzian absorption lineshape (Hawthorne 1988; Amthauer et al. 2004; McCammon 2004; Dyar et al. 2006). In Andreozzi et al. (2008), the lowest values

reported are 0.20 mm/s. Moreover, in the two cases where an unconstrained value of 0.20 was obtained (for Fe^{3+} in Y of sample 61Vbh, and for Fe^{2+} in Y3 of sample 65e), the area of the peak was so small (i.e., comparable to the experimental error) that it did not significantly affect the final fit.

2) In Andreozzi et al. (2008), the model proposed by Dyar et al. (1998) was initially adopted: Fe^{2+} doublets were assigned to Y-sites with different nearest-neighbor environments, arbitrarily designated Y1, Y2 and Y3. For most of the samples, this approach worked very well. However, in some cases, the three environments were not easy to be distinguished: e.g., QS value of the doublet assigned to Y1 in sample 61Vbh (2.39 mm/s) was very close to that assigned to Y2 in sample 62ha (2.35 mm/s). An equally acceptable choice would have been labeling both doublets as Y2, but there was not enough information to do it.

3) As repeatedly stressed in Andreozzi et al. (2008), the assignment of Fe^{2+} to Y and Z was the result of an integrated approach in which the optimized cation distribution was the fit to chemical, structural and spectroscopic data. In particular, in the cases where Fe^{2+} was assigned to Z, site-scattering results pointed to the presence of Fe at Z and the observed bond lengths suggest that Fe is present as Fe^{2+} rather than as Fe^{3+}. For the same samples, Mössbauer fits required an extra Fe^{2+} doublet after refining Y1, Y2 and Y3: the final assignment of this additional doublet to Fe^{2+} at Z was therefore supported by structural results and led to convergence of all experimental data. In spite of that, Ertl et al. (2012a) focus only on the Mössbauer parameters, which are well known to be insufficient in some cases to discriminate Fe^{2+} site allocation. In detail, they stated that the relatively low QS values of Andreozzi et al. (2008) may be due to oxy-varieties, for which the first coordination sphere of Fe^{2+} at Y and Z is similar. However, the Y and Z sites have different second coordination spheres, different point symmetry and different polyhedral distortion–which yield different QS values (Putnis 1995; Dyar et al. 2006). In addition, sample 61Vbh of Andreozzi et al. (2008) has $^{Z}Fe^{2+}$ without an oxy-component.

4) With respect to the criticism on doublets associated with electron delocalization (ED), namely $Fe^{2.5+}$, the same considerations as point 3) apply. In detail, Andreozzi et al. (2008) specified that the assignment of ED doublets to Y-Z, Y-Y or Z-Z is not based on spectral evidence, but on cation distribution derived from single-crystal structure refinement.

5) The criticism regarding the occurrence of $Fe^{2.5+}$ only in a spectrum with the simultaneous presence of Fe^{3+} is hypothetically acceptable only assuming a random cation distribution. However, this seems to be in contrast to the experimental evidence. For example, the Mössbauer spectrum of sample L2al (Andreozzi et al. 2008) shows only $Fe^{2.5+}$ without the simultaneous presence of Fe^{3+}. An alternative interpretation of this spectrum is not reliable because clear evidence of Fe^{3+} was not observed, and the refined $Fe^{2.5+}$ quadrupole doublet has the typical center shift value of ED doublets (0.73 mm/s).

6) Again, the criticism on the supposed impossibility of ED between two adjacent Z sites is based on the hypothesis of a random cation distribution, and is not supported by experimental evidence. What is important for ED is the distance of the two cation sites, which is smaller in Z-Z than in Y-Z and Y-Y. In this regard, a good example of a non-random association of different-valence cations is given by blue sapphire, where trace amounts of Ti^{4+} and Fe^{2+} form locally associated Fe^{2+}-Ti^{4+} pairs responsible for the blue color.

7) Finally, the criticism on the absence of $Fe^{2.5+}$ when high amounts of Fe^{3+} are present is again a speculation not supported by experimental evidence.

Mn^{2+}-RICH TOURMALINE

Ertl et al. (2012a) present several critical comments on the proposed occupancy of 0.08(2) apfu of Mn^{2+} at the Z site in a tourmaline sample (Bosi et al. 2005b). We find this rather excessive as the proposed amount of Mn^{2+} at Z is very small: about 1% atoms/site.

Ertl et al. (2012a) stated that the structural data for Mn-rich tourmalines of Bosi et al. (2005b) are affected by large errors due to the release of the multiplicity of all cation sites (X, Y, Z, T, B) at the same time during the refinement, which could lead to significant correlations between site occupancy and scale factor. Such a statement would be correct only if significant correlations were observed, as listed in the SHELX.LST file (Sheldrick 2008). Bosi et al. (2005b), however, did not observe any of such correlations. Conversely, Bosi et al. (2012) demonstrated that the simultaneous refinement of a large portion of the total scattering is possible in the tourmaline structure if no correlation between site occupancy and scale factor occurs. In fact, a new refinement of sample Tsl2g of Bosi et al. (2005b) was done by Bosi et al. (2012b) constraining the site occupancy of T- and B-sites to 1. Results showed no significant difference with respect to the previous refinement. As a conclusion, the arguments used by Ertl et al. (2012a) against the data of Bosi et al. (2005b) can be ruled out.

Ertl et al. (2012a) also stated that the observed <Z-O> distance of Mn-bearing tourmalines can vary as a function of the Y-cation population, which could accommodate atoms with ionic radius from 0.535 Å (i.e., $^{[6]}Al$) to 0.83 Å (i.e., $^{[6]}Mn^{2+}$). Using the structural data of Mn-bearing tourmalines reported in Bosi et al. (2005b), Ertl et al. (2012a) showed that there is a positive correlation between the Mn^{2+}_{total} and <Z-O>, which can be extrapolated to a value of 1.902 Å for Mn^{2+}-free tourmalines (Fig. 1a). However, such an extrapolation does not work when a real Mn^{2+}-free tourmaline (Elb2rim) is added to the plot (Fig. 1a). Notably, sample Elb2rim comes from the same macrocrystal as the fragments of the Mn-rich tourmalines. The quadratic form of the new correlation obtained suggests the occurrence of cations larger than Al at the Z site. This quadratic trend is further confirmed by considering a larger dataset of 48 Mn-bearing tourmalines (Table 3) with amounts of Mn larger than 0.1 apfu and ^{Z}Al = 6.00 apfu (Fig. 1b). However, it should be noted that that the correlation between <Z-O> and Mn^{2+}_{total} disappears when the standard errors associated with the observed bond distances are taken into account. The observed variation in <Z-O> is within a 3σ uncertainty.

As every experimental measurement is always affected by uncertainty, Hazen and Finger (1982) recommended calculating the standard error of a mean bond length as the average of standard errors (σ) from single bond lengths: e.g., $\sigma_{<Z\text{-}O>} = (\Sigma\sigma_{single\ length})/6$. This procedure, used for example by Shannon et al. (1975) and Shannon (1976), is adopted here. In normal probability theory, two parameters are significantly different if $S = \Delta/(\sigma_1^2+\sigma_2^2)^{1/2} > 3$, where Δ is the difference between the two parameters, and σ_1 and σ_2 are their errors. By applying this procedure to the smallest and largest <Z-O> values [samples T15 and NP1, 1.902(2) Å and 1.910(2) Å, respectively, Burns et al. 1994], with the Z site fully occupied by Al, *S* less than 3 (2.67) is obtained, that is to say these two distances are not distinguishable statistically. As a general conclusion, in Mn-bearing tourmalines there exists no solid evidence for the occurrence of Mn^{2+} at Z or for inductive effects of $^{Y}Mn^{2+}$ on <Z-O>, but just speculative models can be proposed.

VARIATION IN <^{Z}AL-O> DISTANCE

Ertl et al. (2012a) suggested that the out-of-fit plot of Mn^{2+}-free elbaite sample Elb2rim with respect to their linear relation <Z-O> vs. Mn^{2+}_{total} was due to *"inductive effect of different Y-site and maybe also T-site populations"*. In fact, they interpreted the apparent variation of <^{Z}Al-O> distance from 1.902 to 1.913 Å in a dataset of 54 tourmaline as due to inductive effects of <Y-O> and <T-O> on <^{Z}Al-O>. Their main argument for this model was the

correlation between <T-O> and $<^{Z}$Al-O> observed by Ertl et al. (2010a, 2012b) and by multiple regression relations between $<^{Z}$Al-O> vs. different Y-site occupants. The argument will be analyzed from random error perspective (see below), although systematic error may also have a certain relevance (see Appendix 2).

Inductive effect of <T-O> on <Z-O>

Ertl et al. (2010a, 2012b) stated that the influence of <T-O> on the $<^{Z}$Al-O> distance can be calculated as $<^{Z}$Al-O> = [(<T-O>$_{meas.}$ + 1.0439)/1.3961]. A good test to check the accuracy of this relation is given by the olenite sample of Marler et al. (2002), which has a composition …$^{Z}(Al)_6{}^{T}(Si_{3.8}B_{2.2})$… and the smallest observed <T-O> distance (1.573 Å). Using the relation proposed by Ertl et al. (2012b) a calculated $<^{Z}$Al-O> = 1.874 Å is obtained. This value is far less than 1.908 Å observed by Marler et al. (2002).

As for the relation between <T-O> and $<^{Z}$Al-O>, we used a larger dataset (with 110 samples instead of 54, Table 3) than Ertl et al. (2012b). It is evident from the plot of $<^{Z}$Al-O> vs. <T-O> (Fig. 2) that the correlation between the parameters is extremely poor (the determination coefficient drops to $r^2 = 0.34$ from $r^2 = 0.62$, when comparing with Figure 8a of Ertl et al. 2012b) and that the variation in $<^{Z}$Al-O> is within the experimental error (3σ). In fact, a simple statistical analysis shows that the $<^{Z}$Al-O> average value, calculated from the present dataset, is 1.906(2) Å and such a value is consistent with the observed $<^{Z}$Al-O> values at the 99% confidence limit (3σ). As a conclusion, inductive effect of <T-O> on <Z-O> can be ruled out, and $<^{Z}$Al-O> values ranging from 1.900 to 1.912 Å can be considered as statistically equal in tourmalines with the Z site fully occupied by Al.

Inductive effect of <Y-O> on <Z-O>

As for the multiple regression relation between <Y-O> and $<^{Z}$Al-O> proposed by Ertl et al. (2012a), there are several issues related to the dataset used. Ertl et al. (2012a) used 54 samples, but they gave no explanation for the exclusion of samples such as those of Kahlenberg and Veličkov (2000) and Aurisicchio et al. (1999) with the Z site fully occupied by Al, whereas they used samples with the Z site not fully occupied by Al (5.92 apfu) such as those of Hughes et al. (2000) and Bosi et al. (2005b). Again, no explanation was given for the use of <Z-O> = 1.908 Å for the sample of Gorskaya et al. (1982), who instead reported <Z-O> = 1.898 Å.

Ertl et al. (2012a) stated that the correlation between <Y-O> and <Z-O> is displayed in Fig. 11 of Ertl et al. (2010b), here re-plotted in Figure 3a. What is immediately noticeable from this figure is the small number of samples used (five). A far larger number of tourmalines with ^{Z}Al = 6 apfu can be used (110 samples, Table 3) for a plot of <Y-O> against <^{Z}Al-O> (Fig. 3b). The extremely poor correlation (r^2 = 0.08) between these parameters is immediately evident from this figure, and furthermore it is obvious that any variation in <^{Z}Al-O> is random and can be satisfactorily explained by an experimental error (within 3σ) around a mean value of <^{Z}Al-O> = 1.906(2) Å.

A detailed analysis of polyhedral distortions shows that the global distortion of the ZO_6 polyhedron is smaller than that of YO_6: mean quadratic elongation (<λ>) ranges from 1.012 to 1.018 for ZO_6 and from 1.017 to 1.030 for YO_6 (Bosi and Lucchesi 2007). Bosi et al. (2010) showed that <λ> can change as a function of both the bond-angle distortion and bond-length distortion. In accord with the distortion theorem of bond-valence theory (Brown 2002), the bond-length distortion increases with increasing mean bond length. Brown (2006) proposed a parameter to measure the bond-length distortion and, then, to quantify (in Å) the increase in the mean bond length: $\Delta R = -(0.37/N)\ \Sigma\ln(s_i/s')$, where N is the number of bonds formed by the central atom, s_i is the valence of the ith bond and s' is the average valence of the bonds in the coordination sphere ($\Sigma s_i/N$). ΔR reflects, via bond valences, the deviation of the bond lengths from their average value (D') found in a polyhedron with undistorted bond distances. As a result, the mean-bond distance in the observed distorted polyhedron can be expressed as $\langle D \rangle_{obs} = (D' + \Delta R \pm \sigma)$. The calculated ΔR values for tourmalines with ^{Z}Al = 6.00 apfu ($^{Z}\Delta R$) vary from 0.001 to 0.003 Å, which are clearly too small to account for the variation in <^{Z}Al-O> (~0.012 Å) observed in tourmalines. Consequently, there is no evidence to indicate any inductive effects of variation in <^{Z}Al-O>.

Acknowledgments

We sincerely thank Ulf Hålenius, I. David Brown, Howard D. Flack, and Frank C. Hawthorne for useful and instructive suggestions.

References cited

Amthauer, G., Grodzicki, M., Lottermoser, W., and Redhammer, G. (2004) Mossbauer spectroscopy: Basic Principles *in* Spectroscopic Methods in Mineralogy, A. Beran and E. Libowitzky eds., EMU Notes in Mineralogy 6, 345-367.

Andreozzi, G.B., Bosi, F., and Longo, M. (2008) Linking Mössbauer and structural parameters in elbaite-schorl-dravite tourmalines. American Mineralogist, 93, 658–666.

Aurisicchio, C., Demartin, F., Ottolini, L., and Pezzotta, F. (1999) Homogeneous liddicoatite from Madagascar: a possible reference material? First EMPA, SIMS and SREF data. European Journal of Mineralogy, 11, 237–242.

Baksheev, I.A., Chitalin, A.F., Yapaskurt, V.O., Vigasina, M.F., Bryzgalov, I.A. and Ustinov V.I. (2010) Tourmaline in the Vetka porphyry copper-molybdenum deposit of the Chukchi Peninsula of Russia. Moscow University Geology Bulletin, 65, 27–38.

Bloodaxe, E.S., Hughes, J.M., Dyar, M.D., Grew, E.S., and Guidotti, C.V. (1999) Linking structure and chemistry in the schorl-dravite series. American Mineralogist, 84, 922–928.

Bosi, F. (2008) Disordering of Fe^{2+} over octahedrally coordinated sites of tourmaline. American Mineralogist, 93, 1647-1653.

Bosi, F. (2010) Octahedrally coordinated vacancies in tourmaline: a theoretical approach. Mineralogical Magazine, 74, 1037-1044.

Bosi, F. (2011) Stereochemical constraints in tourmaline: from a short-range to a long-range structure. Canadian Mineralogist, 49, 17-27.

Bosi, F. and Lucchesi, S. (2004) Crystal chemistry of the schorl-dravite series. European Journal of Mineralogy, 16, 335–344.

Bosi, F. and Lucchesi, S. (2007) Crystal chemical relationships in the tourmaline group: structural constraints on chemical variability. American Mineralogist, 92, 1054-1063.

Bosi, F., Andreozzi, G.B., Federico, M., Graziani, G., and Lucchesi, S. (2005a) Crystal chemistry of the elbaite-schorl series. American Mineralogist, 90, 1784–1792.

Bosi, F., Agrosì, G., Lucchesi, S., Melchiorre, G., and Scandale, E. (2005b) Mn-tourmaline from island of Elba (Italy): Crystal chemistry. American Mineralogist, 90, 1661–1668.

Bosi, F., Hålenius, U., and Skogby, H. (2010) Crystal chemistry of the $MgAl_2O_4$-$MgMn_2O_4$-$MnMn_2O_4$ system: Analysis of structural distortion in spinel and hausmannite-type structures. American Mineralogist, 95, 602–607.

Bosi, F., Reznitskii, L., and Skogby, H. (2012a) Oxy-chromium-dravite, $NaCr_3(Cr_4Mg_2)(Si_6O_{18})(BO_3)_3(OH)_3O$, a new mineral species of the tourmaline supergroup. American Mineralogist, 97, 2024-2030.

456 Bosi, F., Skogby, H., Agrosì, G., and Scandale, E. (2012b) Tsilaisite,
457 $NaMn_3Al_6(Si_6O_{18})(BO_3)_3(OH)_3OH$, a new mineral species of the tourmaline supergroup
458 from Grotta d'Oggi, San Piero in Campo, island of Elba, Italy. American Mineralogist,
459 97, 989-994.
460 Bosi, F., Reznitskii, L., and Sklyarov, E.V. (2013a) Oxy-vanadium-dravite,
461 $NaV_3(V_4Mg_2)(Si_6O_{18})(BO_3)_3(OH)_3O$: crystal structure and redefinition of the "vanadium-
462 dravite" tourmaline. American Mineralogist, 98, 501-505.
463 Bosi, F., Andreozzi, G.B., Skogby, H., Lussier, A.J., Abdu, Y., and Hawthorne, F.C. (2013b)
464 Fluor-elbaite, $Na(Li_{1.5}Al_{1.5})Al_6(Si_6O_{18})(BO_3)_3(OH)_3F$, a new mineral species of the
465 tourmaline supergroup. American Mineralogist, 98, 297-303.
466 Brese, N.E. and O'Keeffe, M. (1991) Bond-valence parameters for solids. Acta
467 Crystallographica, B47, 192.197.
468 Brown, I.D. (2002) The chemical bond in inorganic chemistry: the bond valence model.
469 International Union of Crystallography Monographs on Crystallography, 12, 288 p.
470 Oxford University Press, U.K.
471 Brown, I.D. (2006) On measuring the size of distortions in coordination polyhedra. Acta
472 Crystallographica, B62, 692–694.
473 Brown, I.D. (2009) Recent Developments in the Methods and Applications of the Bond
474 Valence Model. Chemical Reviews, 109, 6858-6919.
475 Brown, I.D. and Altermatt, D. (1985) Bond-valence parameters obtained from a systematic
476 analysis of the Inorganic Crystal Structure Database. Acta Crystallographica, B41, 244-
477 247.
478 Burns, R.G. (1972) Mixed valencies and site occupancies of iron in silicate minerals from
479 Mössbauer spectroscopy. Canadian Journal of Spectroscopy, 17, 51–59.
480 Burns, P.C., MacDonald, D.J., and Hawthorne, F.C. (1994) The crystal chemistry of
481 manganese-bearing elbaite. Canadian Mineralogist, 32, 31–41.
482 Camargo, M.B. and Isotani, S. (1988) Optical absorption spectroscopy of natural and irradiated
483 pink tourmaline. American Mineralogist, 73,172-180
484 Donnay, G. and Barton, R. Jr. (1972) Refinement of the crystal structure of elbaite and the
485 mechanism of tourmaline solid solution. Tschermaks Mineralogische und
486 Petrographische Mitteilungen, 18, 273-286.

Dyar, M.D., Taylor, M.E., Lutz, T.M., Francis, C.A., Guidotti, C.V., and Wise, M. (1998) Inclusive chemical characterization of tourmaline: Mössbauer study of Fe valence and site occupancy. American Mineralogist, 83, 848–864.

Dyar, M.D., Agresti, D.G., Schaefer, M.W., Grant, C.A., and Sklute, E.C. (2006) Mössbauer spectroscopy of Earth and planetary materials. Annual Review of Earth and Planetary Sciences, 34, 83-125.

Ertl, A. and Hughes, J.M. (2002) The crystal structure of an aluminum-rich schorl overgrown by boron-rich olenite from Koralpe, Styria, Austria. Mineralogy and Petrology, 75, 69-78.

Ertl, A., Hughes, J.M., Prowatke, S., Ludwig, T., Brandstatter, F., Korner, W., and Dyar, M.D. (2007) Tetrahedrally coordinated boron in Li-bearing olenite from "Mushroom" tourmaline from Momeik, Myanmar. Canadian Mineralogist, 45, 891-899.

Ertl, A., Tillmans, E., Ntaflos, T., Francis, C., Giester, G., Körner, W., Hughes, J.M., Lengauer, C., and Prem, M. (2008) Tetrahedrally coordinated boron in Al-rich tourmaline and its relationship to the pressure-temperature conditions of formation. European Journal of Mineralogy, 20, 881-888.

Ertl, A., Hughes, J.M., and Tillmanns, E. (2010a) The correct formula for Mg- and Fe3+-tourmaline: the influence of the <T-O> distance on the <Z-O> bond length. Acta Mineralogica-Petrographica Abstract Series, Volume 6, 476, IMA2010 20th General Meeting of the International Mineralogical Association, 21–27 August 2010, Budapest, Hungary.

Ertl, A., Rossman, G.R., Hughes, J.M., London, D., Wang, Y., O'Leary, J.A., Dyar, M.D., Prowatke, S., Ludwig, T., and Tillmanns, E. (2010b) Tourmaline of the elbaite-schorl series from the Himalaya Mine, Mesa Grande, California, U.S.A.: A detailed investigation. American Mineralogist, 95, 24–40.

Ertl, A., Kolitsch, U., Dyar, M.D., Hughes, J. M., Rossman, G.R., Pieczka, A., Henry, D. J., Pezzotta, F., Prowatke, S., Lengauer, C.L., Körner, W., Brandstatter, F., Francis, C.A., Prem, M., and Tillmans, E. (2012a) Limitations of Fe^{2+} and Mn^{2+} site occupancy in tourmaline: evidence from Fe^{2+}- and Mn^{2+}-rich tourmaline. American Mineralogist, 97, 1402-1416.

Ertl, A., Schuster, R., Hughes, J.M., Ludwig, T., Meyer, H.-P., Finger, F., Dyar, M.D., Ruschel, K., Rossman, G.R., Klötzi, U., Brandstätter, F., Lengauer, C.L., Tillmans, E.

(2012b) Li-bearing tourmalines in Variscan granitic pegmatites from the Moldanubian nappes, Lower Austria. European Journal of Mineralogy, 24, 695-715.

Ertl, A., Giester, G., Ludwig, T., Meyer, H.P., and Rossman, G.R. (2012c) Synthetic B-rich olenite: Correlations of single-crystal structural data. American Mineralogist, 97, 1591-1597.

Ertl, A., Giester, G., Schüssler, U., Brätz, H., Okrusch, M., Tillmanns, E., and Bank, H. (2013) Cu- and Mn-bearing tourmalines from Brazil and Mozambique: Crystal structures, chemistry and Correlations. Mineralogy and. Pertrology, DOI 10.1007/s00710-012-0234-6.

Ferrow, E.A. (1994) Mössbauer effect study of the crystal chemistry of tourmaline. Hyperfine Interactions, 91, 689–695.

Ferrow, E.A., Annersten, H., and Gunawardane, R.P. (1988) Mössbauer effect study on the mixed valence state of iron in tourmaline. Mineralogical Magazine, 52, 221–228.

Ferrow, E.A., Wallenberg, L.R. and Skoghy, H. (1993) Compositional control of plane group symmetry in tourmalines: an experimental and computer simulated TEM, crystallographic image processing and Mössbauer spectroscopy study. European Journal of Mineralogy, 5, 479-492.

Filip, J., Bosi, F., Novák, M., Skogby, H., Tuček, J., Čuda, J., and Wildner, M. (2012) Redox processes of iron in the tourmaline structure: example of the high-temperature treatment of Fe^{3+}-rich schorl. Geochimica et Cosmochimica Acta, 86, 239–256.

Flack, H.D. and Bernardinelli, G. (2000) Reporting and evaluating absolute-structure and absolute-configuration determinations. Journal of Applied Crystallography, 33, 1143-1148.

Foit, F.F. Jr. (1989) Crystal chemistry of alkali-deficient schorl and tourmaline structural relationships. American Mineralogist, 74, 422-431.

Foit Jr., F.F., Fuchs, Y., and Myers, P.E. (1989) Chemistry of alkali-deficient schorls from two tourmaline-dumortierite deposits. American Mineralogist, 74, 1317–1324.

Fortier, S. and Donnay, G. (1975) Schorl refinement showing composition dependence of the tourmaline structure. Canadian Mineralogist, 13, 173–177.

Francis, C.A., Dyar, M.D., Williams, M.L., and Hughes, J.M. (1999) The occurrence and crystal structure of foitite from a tungsten-bearing vein at Copper Mountain, Taos County, New Mexico. Canadian Mineralogist, 37, 1431–1438.

Fuchs, Y., Lagache, M., Linares, J., Maury, R., and Varret, F. (1995) Mössbauer and optical spectrometry of selected schorl-dravite tourmalines. Hyperfine Interactions, 96, 245–258.

Fuchs, Y., Lagache, M., and Linares, J. (1998) Fe-tourmaline synthesis under different T and f_{O2} conditions. American Mineralogist, 83, 525-534.

Gadas, P., Novák, M., Staněk, J., Filip, J., and Vašinová Galiová, M. (2012) Compositional Evolution of Zoned Tourmaline Crystals from Pockets in Common Pegmatites of the Moldanubian Zone, Czech Republic. Canadian Mineralogist, 50, 895-912.

Gatta, G.D., Danisi, R.M., Adamo, I., Meven, M., and Diella, V. (2012) A singlecrystal neutron and X-ray diffraction study of elbaite. Physics and Chemistry of Minerals, 39, 577-588.

Gorskaya, M.G., Frank-Kamenetskaya, O.V., Rozhdestvenskaya, I.V., and Frank-Kamenetskii, V.A. (1982) Refinement of the crystal structure of Al-rich elbaite, and some aspects of the crystal chemistry of tourmalines. Soviet Physics Crystallography, 27, 63–66.

Grice, J.D. and Robinson, G.W. (1989) Feruvite, a new member of the tourmaline group, and its crystal structure. Canadian Mineralogist, 27, 199–203.

Grice, J.D. and Ercit, T.S. (1993) Ordering of Fe and Mg in the tourmaline crystal structure: the correct formula. Neues Jahrbuch für Mineralogie, Abhandlungen, 165, 245-266.

Hawthorne, F.C. (1988) Mössbauer Spectroscopy *in* Spectroscopic Methods in Mineralogy and Geology, F.C. Hawthorne editor, Reviews in Mineralogy, 18, 255-340.

Hawthorne, F.C. (1996) Structural mechanisms for light-element variations in tourmaline. Canadian Mineralogist, 34, 123-132.

Hawthorne, F.C. (2002) Bond-valence constraints on the chemical composition of tourmaline. Canadian Mineralogist, 40, 789–797.

Hawthorne, F.C. and Henry, D. (1999) Classification of the minerals of the tourmaline group. European Journal of Mineralogy, 11, 201-215.

Hawthorne, F.C., MacDonald, D.J., and Burns, P.C. (1993) Reassignment of cation site-occupancies in tourmaline: Al-Mg disorder in the crystal structure of dravite. American Mineralogist, 78, 265–270.

Hazen, R.M., and Finger, L.W. (1982) Comparative crystal chemistry. Wiley, New York.

Henry, D.J. and Dutrow, B.L. (1996) Metamorphic tourmaline and its petrologic applications. In L.M. Anovitz and E.S. Grew, Eds., Boron: Mineralogy, Petrology and Geochemistry,

33, p. 503–557. Reviews in Mineralogy, Mineralogical Society of America, Chantilly, Virginia.

Henry, D.J., Novák, M., Hawthorne, F.C., Ertl, A., Dutrow, B., Uher, P., and Pezzotta, F. (2011) Nomenclature of the tourmaline supergroup minerals. American Mineralogist, 96, 895-913.

Hermon, E., Simkin, D.J. and Donnay, G. (1973) The distribution of Fe^{2+} and Fe^{3+} in iron-bearing tourmalines: A Mössbauer study. Tschermaks Mineralogische und Petrographische Mitteilungen, 19, 124-132.

Hughes, J.M., Ertl, A., Dyar, M.D., Grew, E., Shearer, C.K., Yates, M.G., and Giudotti, C.V. (2000) Tetrahedrally coordinated boron in a tourmaline: Boron-rich olenite from Stoffhütte, Koralpe, Austria. Canadian Mineralogist, 38, 861–868.

Kahlenberg, V. and Veličkov, B. (2000) Structural investigations on a synthetic alkali-free hydrogen-deficient Fe-tourmaline (foitite). European Journal of Mineralogy, 12, 947-953.

Kihara, K., Hirata, H., Ida, A., Okudera, H., and Morishita, T. (2007) An X-ray single crystal study of asymmetric thermal vibrations and the positional disorder of atoms in elbaite. Journal of Mineralogical and Petrological Sciences, 102, 115-126.

Korovushkin, V.V., Kuzmin, V.I. and Belov, V.F. (1979) Mössbauer studies of structural features in tourmaline of various genesis. Physics and Chemistry of Minerals, 4, 209-20.

Kraczka, J., Pieczka, A., Hrynkiewicz, A.Z. and Zabiński, W. (1986) Mo□ssbauer study of tourmalines. Hyperfine Interactions 29, 1121-1124.

Kraczka, J. and Pieczka, A. (2000) Mössbauer study of thermal oxidation of Fe^{2+} in tourmaline. Molecular Physics Reports, 30, 80-85.

Lussier, A.J. (2011) Zonation in Tourmaline From Granitic Pegmatites and The Occurence of Tetrahedrally Coordinated Aluminum and Boron in Tourmaline. Ph.D. thesis, University of Manitoba, Winnipeg, Manitoba.

Lussier, A.J., Aguiar, P.M., Michaelis, V.K., Kroeker, S., Herwig, S., Abdu, Y., and Hawthorne, F.C. (2008) Mushroom elbaite from the Kat Chay mine, Momeik, near Mogok, Myanmar: I. Crystal chemistry by SREF, EMPA, MAS NMR and Mössbauer spectroscopy. Mineralogical Magazine, 72, 747-761.

Lussier, A.J., Hawthorne, F.C., Abdu, Y., Herwig, S., Michaelis, V.K., Aguiar, P.M., and Kroeker, S. (2011a) The crystal chemistry of `wheatsheaf' tourmaline from Mogok, Myanmar. Mineralogical Magazine, 72, 999-1010.

615 Lussier, A.J., Abdu, Y. Hawthorne, F.C., Michaelis, V.K., Aguiar, P.M., and Kroeker, S.
616 (2011b) Oscillatory zoned liddicoatite from Anjanabonoina, central Madagascar. I.
617 Crystal chemistry and structure by SREF and 11B and 27Al MAS NMR spectroscopy.
618 Canadian Mineralogist, 49, 63-88.
619 Marler, B., Borowski, M., Wodara, U., and Schreyer, W. (2002) Synthetic tourmaline (olenite)
620 with excess boron replacing silicon in the tetrahedral site: II. Structure analysis.
621 European Journal of Mineralogy, 14, 763–771.
622 Mattson, S.M. and Rossman, G.R. (1984) Ferric iron in tourmaline. Physics and Chemistry of
623 Minerals, 14, 225-234.
624 Mattson, S.M. and Rossman, G.R. (1987) Fe^{2+}-Fe^{3+} interactions in tourmaline. Physics and
625 Chemistry of Minerals, 14, 163-171.
626 McCammon C.A. (2004). Mossbauer spectroscopy: Applications *in* Spectroscopic Methods in
627 Mineralogy, A. Beran and E. Libowitzky eds., EMU Notes in Mineralogy 6, 369-398.
628 Nuber, B. and Schmetzer, K. (1979) Die Gitterposition des Cr^{3+} im Turmalin:
629 Strukturverfeinerung eines Cr-reichen Mg-Al-Turmalins. Neues Jahrbuch für
630 Mineralogie Abhandlungen, 137, 184-197.
631 Pieczka, A. (1997) Statistical interpretation of structural parameters of tourmaline iron ordering
632 in octahedral sites. Tourmaline 1997 International Symposium on Tourmaline, Nové
633 Mesto na Morave, Czech Republic, 70–71.
634 Pieczka, A. and Kraczka, J. (1997) Thermal oxidation of Fe2+ ions in the schorl-dravite series
635 and its significance in the analysis of distribution of Fe2+ octahedral ions. Tourmaline
636 1997 International Symposium on Tourmaline, Nové Mesto na Morave, Czech Republic,
637 72–73.
638 Pieczka, A. and Kraczka, J. (2001) X-ray and Mössbauer study of Fe^{2+} thermal oxidation in Fe-
639 Mg-Al-tourmaline. Bulletin Liaison S.F.M.C., 13, 42-43.
640 Pieczka, A. and Kraczka, J. (2004) Oxidized tourmalines—a combined chemical, XRD and
641 Mössbauer study. European Journal of Mineralogy, 16, 309–321.
642 Putnis, A. (1995) Introduction to Mineral Sciences, 457 p. Cambridge University Press.
643 Razmanova, Z.P., Kornetova, V.A., Shipko, M.N. and Belov, N.V. (1983) Refinements in
644 crystal structure and configuration of iron-bearing uvite. Trudy AN SSSR,
645 Mineralogicheskiy Muzey im. A.E. Fersmana 31, 108-116 (in Russian).
646 Shannon, R.D. (1976) Revised effective ionic radii and systematic studies of interatomic
647 distances in halides and chalcogenides. Acta Crystallographica, A32, 751.767.

Shannon, R.D., Gumerman, P.S., and Chenavas, J. (1975) Effect of octahedral distortion on mean Mn^{3+}-O distances. American Mineralogist, 60, 714–716.

Sheldrick, G.M. (2008) A short history of SHELX. Acta Crystallographica, A, 64, 112–122.

Smith, G. (1978) A reassessment of the role of iron in the 5,000–30,000 cm^{-1} region of the electronic absorption spectra of tourmaline. Physics and Chemistry of Minerals, 3, 343–373.

Taran, M.N., Lebedev, A.S., and Platonov, A.N. (1993) Optical absorption spectroscopy of synthetic tourmalines. Physics and Chemistry of Minerals, 20, 209-220.

Wright, S.E., Foley, J.A., and, Hughes, J.M. (2000) Optimization of site occupancies in minerals using quadratic programming. American Mineralogist, 85, 524-531.

659
660 **LIST OF TABLES**

661 **TABLE 1.** Structural studies reporting Fe^{2+} at Z from the literature (before 2004).

662 **TABLE 2.** Sample BSL1 of Ertl et al. (2012a): site populations of Y and Z (apfu), mean atomic
663 number (m.a.n), mean bond distance (m.b.d.), bond valence sum (BVS), and mean
664 formal valence (MFV).

665 **TABLE 3.** References of tourmalines having the Z site population consistent with the
666 occurrence of Al.

667
668 **LIST OF FIGURES AND FIGURE CAPTIONS**

669 **FIGURE 1.** Variation in <Z-O> as a function of the Mn^{2+} content in tourmalines with Z site
670 population consistent with the occurrence of Al: plot obtained by using (a) 7
671 samples coming from the same macrocrystal, (b) 48 samples with Mn > 0.01 apfu.
672 Dotted line shows the linear fit obtained by Ertl et al. (2012a) using 6 samples with
673 Mn > 0.80 apfu. Solid and dashed lines show the quadratic fit obtained using 7 and
674 48 samples, respectively (see text). Black circles = data from Bosi et al. (2005b);
675 white circles = data from Table 3.

676 **FIGURE 2.** Plot of $<^{Z}$Al-O> vs. <T-O> in tourmalines having the Z site population consistent
677 with the occurrence of Al. The horizontal solid line represents the $<^{Z}$Al-O> average
678 value (1.906 Å) for 110 data found in the literature (see Table 3), the two dashed
679 lines represent ±3σ departure from $<^{Z}$Al-O>.

680 **FIGURE 3.** Plot of $<^{Z}$Al-O> vs. <Y-O> in tourmalines having Z-sites having the Z site
681 population consistent with the occurrence of Al: plot obtained using (a) the data
682 reported in Fig. 11 of Ertl et al. (2010b), (b) 110 data found in the literature (see
683 Table 3). The horizontal solid line represents the $<^{Z}$Al-O> average value (1.906 Å),
684 the two dashed lines represent ±3σ departure from $<^{Z}$Al-O>.

685
686
687 **APPENDIX 1. ASSIGNMENT OF Ti^{4+} TO THE Y AND Z SITES**

688 Ertl et al. (2012a) present a method for the assignment of Ti^{4+} to the Y or Z sites of
689 tourmaline by calculation of bond-valence sums for the ion at the two sites. They stated that
690 about 0.14 apfu of Ti^{4+} occurs at the Z site in sample BLS1 because Ti^{4+} at the Y site is greatly
691 underbonded (bond-valence sums 3.11 valence units, v.u.), but Ti^{4+} at the Z site is close to its

formal valence (bond-valence sums 4.29 v.u.). They used this method to support the assignment of Ti, Mn and Fe at one of the two octahedrally coordinated sites of tourmaline. However, 1) the interatomic distances are the long-range average and only are relevant to the bond valences calculated with the average site populations (one has no idea of the local Ti-O distances at either of the sites) and 2) the bond-valence method is limited by the experimental uncertainty in bond distance as well as by possible steric strains that, in general, also contribute to deviations from the valence-sum rule. In practice, the accuracy of any determination of occupation numbers by this method is limited to around 10% (I.D. Brown, personal communication). As a consequence, for sample BLS1 this method is obviously not sufficiently accurate to determine the distribution of Ti^{4+}, because its occupancy is less than 5% for Y sites and smaller than 3% for Z sites.

In accordance with the bond-valence theory (Brown 2002, 2009), however, it is possible to make some predictions on the assignment of Ti^{4+} to the Y or Z site of tourmaline. The Z site would be the most favorable for Ti^{4+} in terms of charge as the valence of 4+ is closer to the ~3+ of the Z site than to the typical ~2+ of the Y site. The valence match of any site to the Ti atom is reflected in the ability of the ligands to accept the 4/6 = 0.67 v.u. Ti^{4+}-O bonds. Clearly the Z site would be better, since it already accepts bonds of 3/6 = 0.5 v.u. while the Y site ligands only accept bonds of valence 2/6 = 0.33 v.u.. Against this, one could argue that although the Y site is too large for the Ti atom, it is possible for Ti to compensate for this in several ways. Firstly, the Ti atom could move away from the center of the cavity. The nature of the bond-valence vs. bond-length correlation shows that such a displacement will increase the bond-valence sum. Notably, Ti^{4+}, being a d^0 transition metal cation, is susceptible to such a distortion. The combination of steric and electronic effects might be sufficient to stabilize Ti in the Y site. In addition, another important factor may come into play: the bond strain. To evaluate this strain, ideal bond lengths for the tourmaline structure should be calculated by solving the network equations for the bond valences (Brown 2002; Bosi and Lucchesi 2007). Mapping the distances calculated in this way into real space may require stretching some bonds and compressing others, so that the measured bond lengths may not be the same as the ideal bond lengths. This strain can often be recognized by the bond-valence sums (BVS) calculated from the experimental bond lengths being too large (compression) or too small (tension) with respect to mean formal valence (MFV). If the Z-O bonds had to be stretched when they were mapped into three dimensions (i.e., giving a weighted bond valence sum for the atoms known to occupy the site that is too small), then substituting Ti would help to relieve the strain since

Ti would help to increase the average bond-valence sum. The same would be true if the Y-O bonds were compressed (weighted bond-valence sum on the site is too large) since Ti would help to lower this sum. If the bonds in both sites were therefore stretched, this would favor substitution on the Z site, and if the bonds on both sites were compressed, the Y site would be favored.

For sample BLS1, the mismatch between BVS and MFV at Y and Z sites was calculated in Table 2, first according to the cation distributions proposed by Ertl et al. (2012a) and then according to the two new optimized formulae. In the first case, the Y site is strongly compressed (BVS – MFV = 0.23) while the Z site is not (BVS – MFV = –0.06), suggesting that Ti^{4+} should accommodate at Y (rather than Z) in order to lower the BVS value and then minimize the observed mismatch. In the other two cases, however, no significant mismatch is observed between BVS and MFV, and consequently the very small Ti amounts may occupy Y or Z without affecting the results.

APPENDIX 2. DECEPTIVE CORRELATIONS IN SREF DATA

Misleading correlations between structural parameters of a crystal structure may appear as an effect of the occurrence of systematic error. Among several types of systematic error, the most invidious are probably those derived from a poorly aligned diffractometer because they are difficult to detect, and lead to a reduction in accuracy in the crystal geometry. A badly aligned diffractometer, in fact, involves systematic errors in 2θ, which lead to a corresponding error in the refined unit-cell parameters and, hence, in bond distances. These latter can assume either smaller or larger values with respect to the correct one. As these errors depend on the diffraction geometry, no indication of them can be seen in the statistical indices of a successful crystal-structure refinement. As a result, an apparent inductive effects of <T-O> (or <Y-O>) on <Z-O> in tourmaline may arise by the occurrence of systematic errors.

TABLE 1. Structural studies reporting Fe^{2+} at Z from the literature (before 2004)

Papers	Z site population (apfu)
Fortier and Donnay (1975)	5.60 Al + **0.40 Fe^{2+}**
Razmanova et al. (1983)	5.00 Al + 0.67 Mg + **0.33 Fe^{2+}**
Grice and Robinson (1989)	4.72 Al + 0.82 Mg + 0.34 Fe^{3+} + **0.12 Fe^{2+}**
Francis et al. (1999)	4.76 Al + 0.18 Mg + **0.06 Fe^{2+}**
Ertl and Hughes (2002)	5.70 Al + 0.20 Mg + **0.08 Fe^{2+}** + **0.02 Mn^{2+}**

TABLE 2. Sample BSL1 of Ertl et al. (2012a): site populations of Y and Z (apfu), mean atomic number (m.a.n), mean bond distance (m.b.d.), bond valence sum (BVS), and mean formal valence (MFV)

Site	Site population	m.a.n. mismatch (observed – calculated)	m.b.d. mismatch* (observed – calculated)	m.b.d. mismatch† (observed – calculated)	(BVS – MFV) mismatch
	Proposed by Ertl et al. (2012a)				
Y	2.02 Fe^{2+} + 0.41 Al + 0.23 Fe^{3+} + 0.32 Mn^{2+} + 0.02 Zn	(23.78 – 24.14) = –0.37	(2.062 – 2.103) = –0.041	(2.062 – 2.103) = –0.041	(2.45 – 2.21) = 0.23
Z	4.82 Al + 0.78 Fe^{3+} + 0.22 Fe^{2+} + 0.14 Ti^{4+} + 0.03 Mg	(15.64 –15.39) = 0.25	(1.941 – 1.930) = 0.011	(1.941 – 1.937) = 0.004	(2.92 – 2.98) = –0.06
	New, optimized using Bosi and Lucchesi (2004, 2007)				
Y	1.31 Fe^{2+} + 0.50 Al + 0.84 Fe^{3+} + 0.32 Mn^{2+} + 0.02 Zn	(23.78 – 23.74) = 0.04	(2.062 – 2.068) = –0.006	(2.062 – 2.064) = –0.002	(2.46 – 2.45) = 0.01
Z	4.73 Al + 0.17 Fe^{3+} + 0.94 Fe^{2+} + 0.14 Ti^{4+} + 0.03 Mg	(15.64 –15.60) = 0.04	(1.941 – 1.947) = –0.006	(1.941 – 1.942) = 0.001	(2.91 – 2.86) = 0.05
	New, optimized using Wright et al. (2000)				
Y	1.27 Fe^{2+} + 0.44 Al + 0.79 Fe^{3+} + 0.31 Mn^{2+} + 0.15 Ti^{4+} + 0.03 Zn + 0.01 Mg	(23.78 – 23.78) = 0.00	(2.062 – 2.066) = –0.004	(2.062 – 2.063) = –0.001	(2.50 – 2.51) = –0.01
Z	4.79 Al + 0.23 Fe^{3+} + 0.98 Fe^{2+}	(15.64 –15.63) = 0.01	(1.941 – 1.948) = –0.007	(1.941 – 1.943) = 0.002	(2.89 – 2.84) = 0.05

Notes: apfu = atoms per formula unit; bond distances in Å; BVS in valence units.
* Calculated from the ionic radii of Shannon (1976), except for <Al-O> for which a distance of 1.906 Å was used (see text).
† Calculated from the ionic radii of Bosi and Lucchesi (2007)

TABLE 3. References of tourmalines having the *Z* site population consistent with the occurrence of Al.

Reference	Sample numbers
Bosi and Lucchesi (2007)	45
Ertl et al. (2007)	1
Kihara et al. (2007)	1
Ertl et al (2008)	1
Lussier et al. (2008)	9
Lussier et al. (2011a)	8
Lussier et al. (2011b)	23
Ertl et al. (2012b)	6
Ertl et al. (2012c)	3
Gatta et al. (2012)	1
Ertl et al. (2013)	8
Bosi et al. (2013b)	2
Bosi et al. (unpublished)	2

Figure 1A

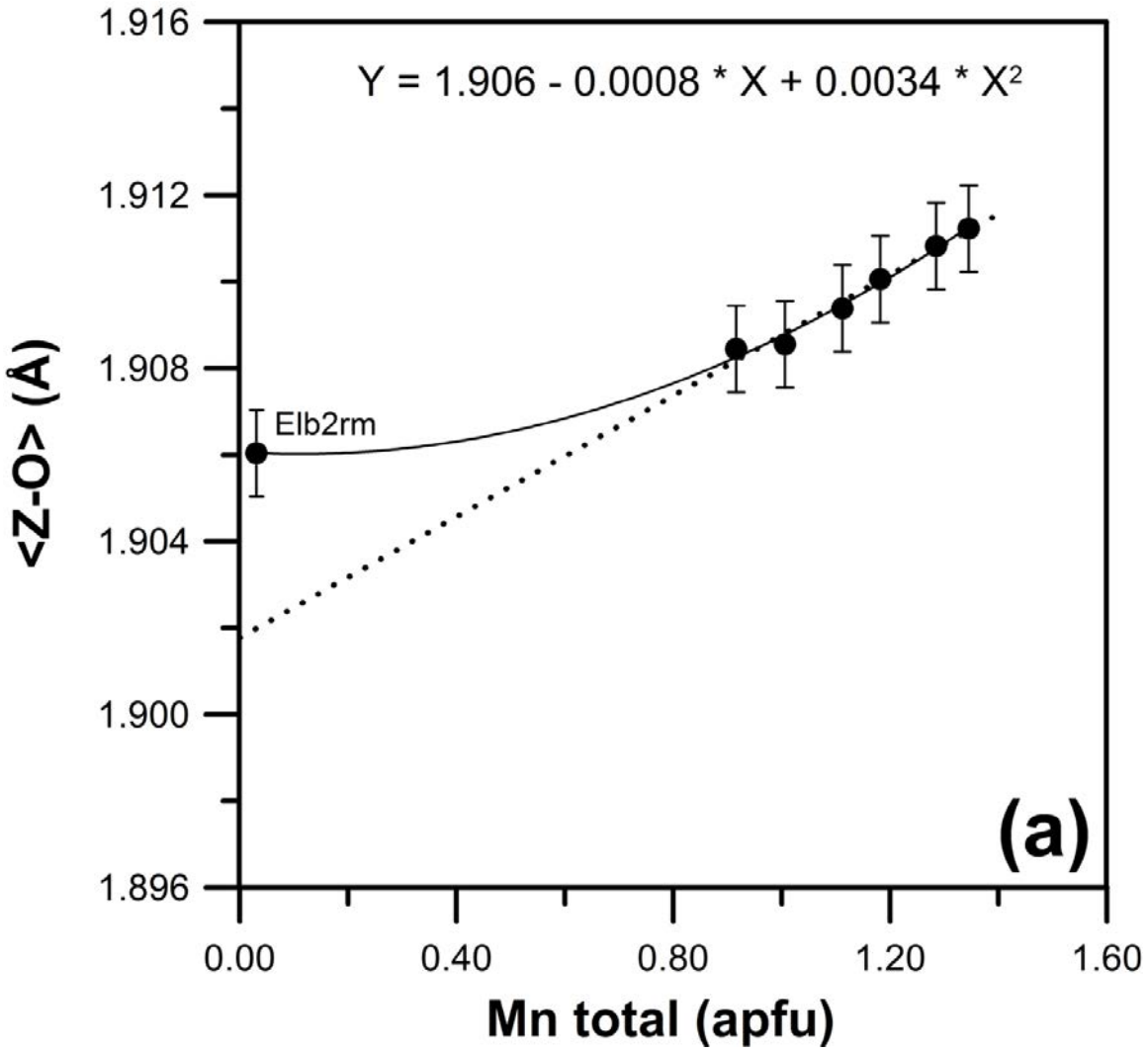
Y = 1.906 - 0.0008 * X + 0.0034 * X²
Elb2rm
(a)
<Z-O> (Å)
Mn total (apfu)
1.916
1.912
1.908
1.904
1.900
1.896
0.00
0.40
0.80
1.20
1.60

Figure 1B

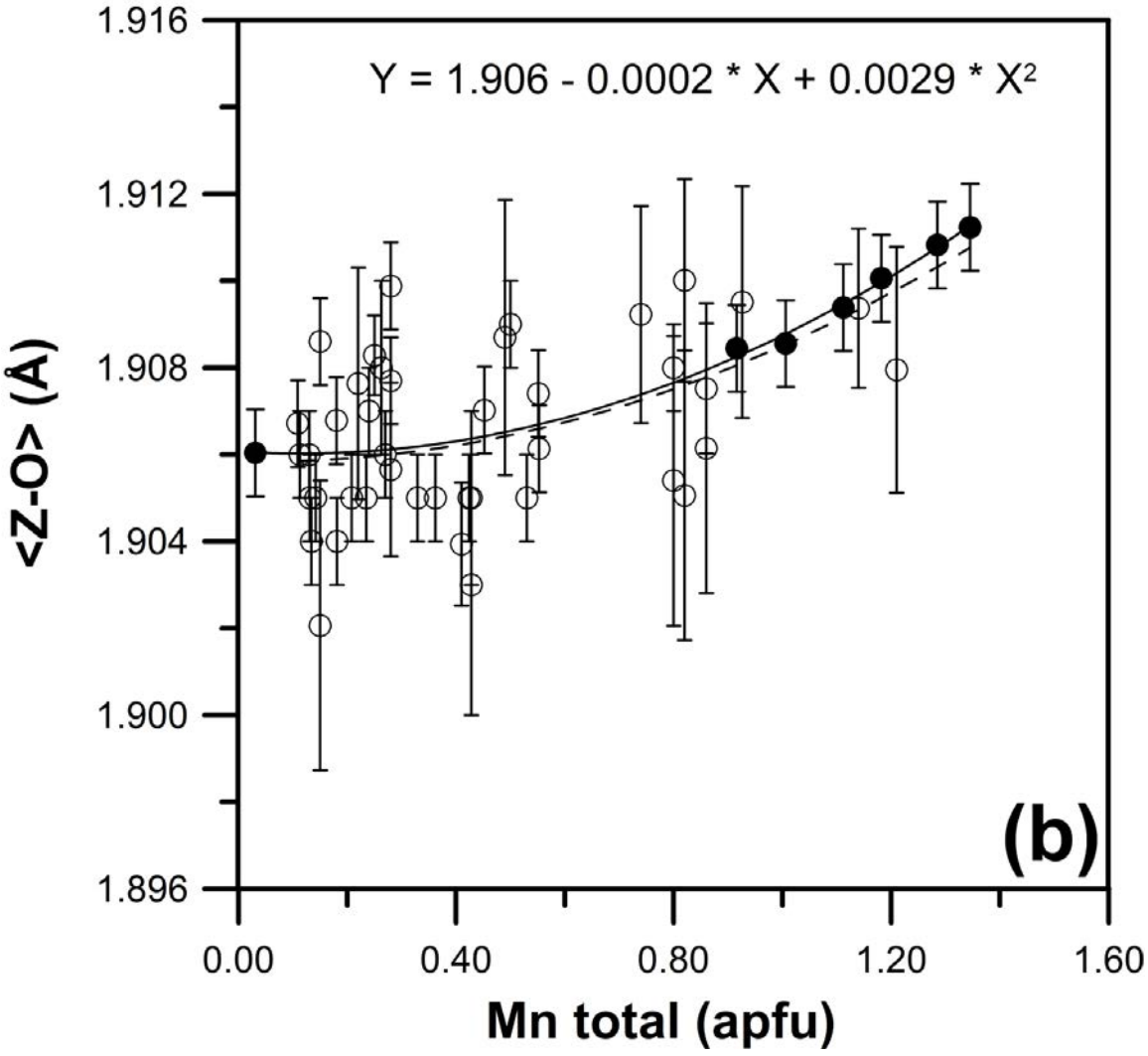
Y = 1.906 - 0.0002 * X + 0.0029 * X²
<Z-O> (Å)
1.916
1.912
1.908
1.904
1.900
1.896
0.00
0.40
0.80
1.20
1.60
Mn total (apfu)
(b)

Figure 2

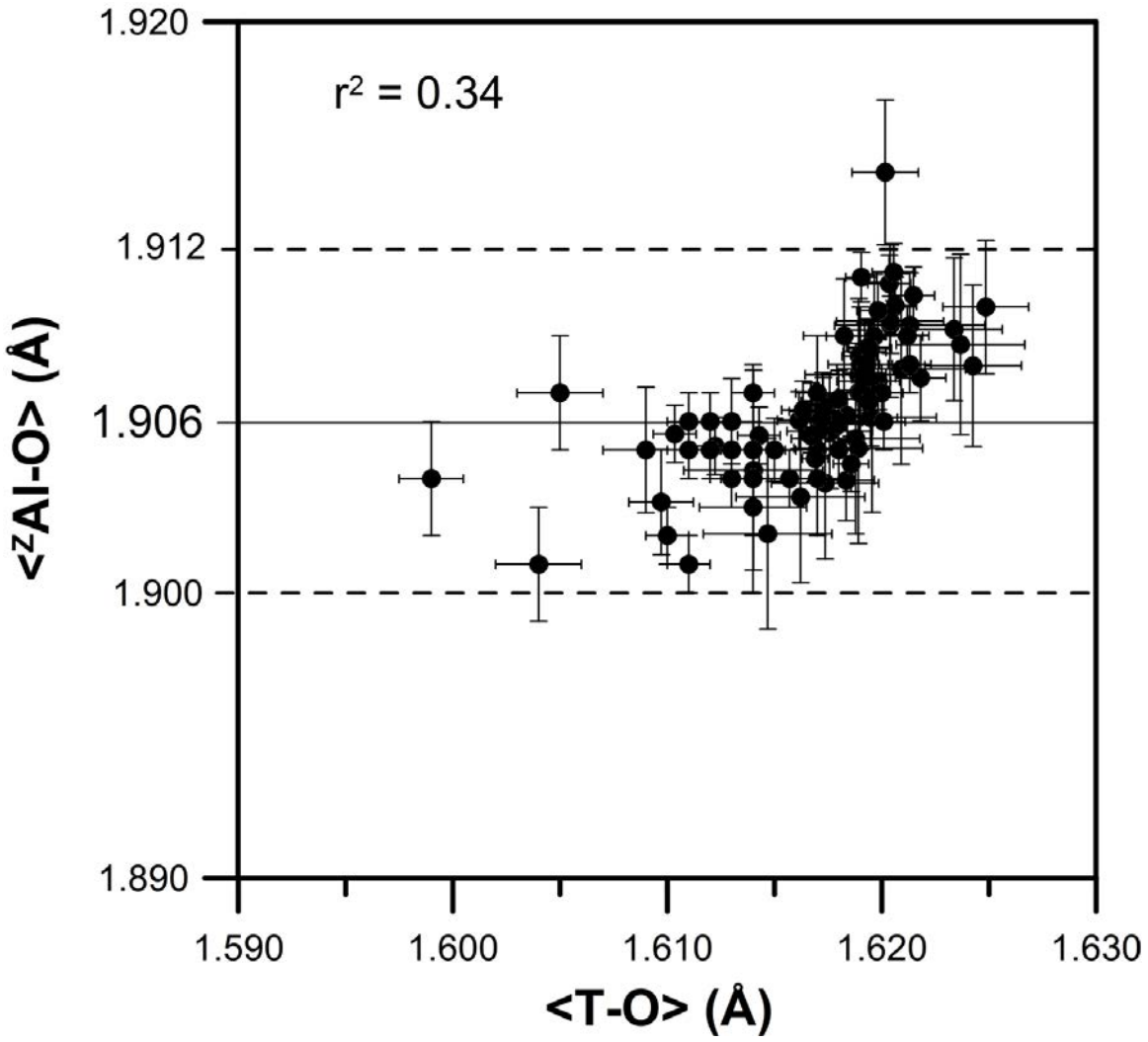
1.920
1.912
1.906
1.900
1.890
r² = 0.34
<ᶻAl-O> (Å)
1.590
1.600
1.610
1.620
1.630
<T-O> (Å)

Figure 3A

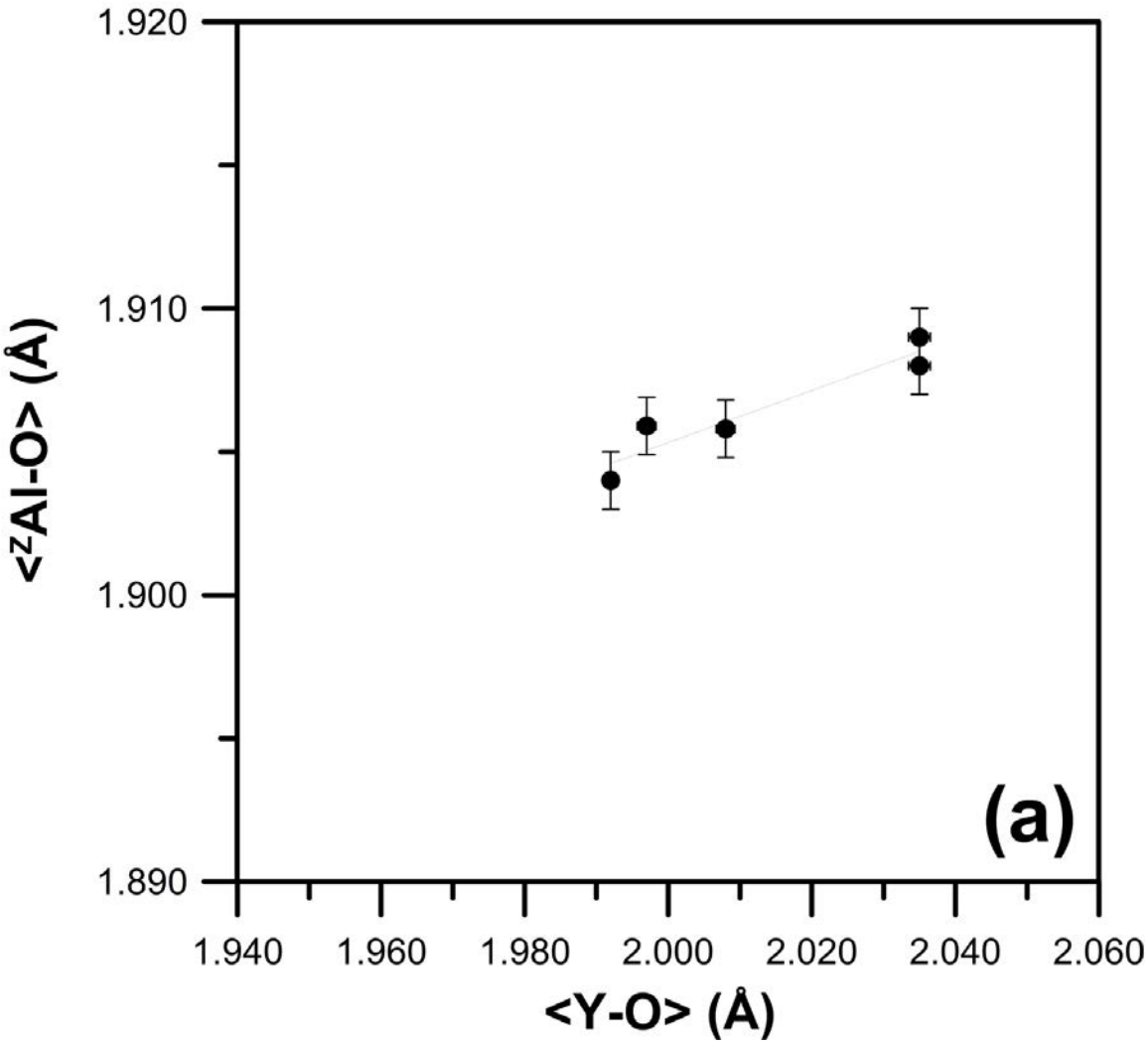
1.920
1.910
1.900
1.890
<zAl-O> (Å)
1.940
1.960
1.980
2.000
2.020
2.040
2.060
<Y-O> (Å)
(a)

Figure 3B

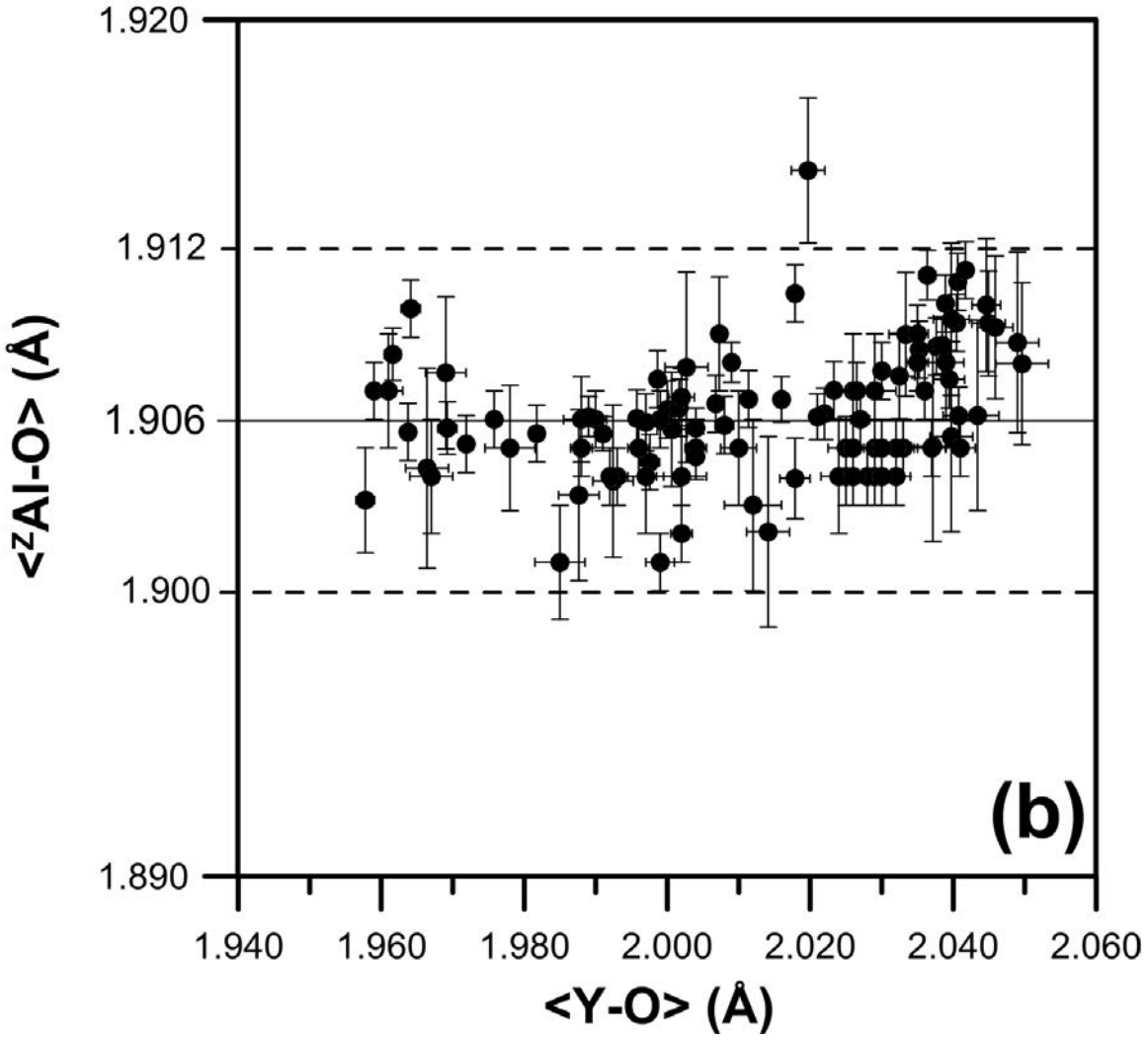
1.920
1.912
1.906
1.900
1.890
<ZAl-O> (Å)
1.940
1.960
1.980
2.000
2.020
2.040
2.060
<Y-O> (Å)
(b)